

Article

Impacts of 1.5 and 2.0 °C Global Warming on Water Balance Components over Senegal in West Africa

Mamadou Lamine Mbaye ^{1,*}, Mouhamadou Bamba Sylla ² and Moustapha Tall ³ 

¹ Laboratoire d'Océanographie, des Sciences de l'Environnement et du Climat (LOSEC), Université Assane, SECK de Ziguinchor BP 523, Senegal

² African Institute for Mathematical Sciences (AIMS), AIMS Rwanda Center, KN 3, P.O. Box 71 50 Kigali, Rwanda; syllabamba@yahoo.fr

³ Laboratoire de Physique de l'Atmosphère et de l'Océan, Ecole Supérieure Polytechnique, Université Cheikh Anta Diop, Dakar BP 5085, Senegal; tall.moustapha89@gmail.com

* Correspondence: mlmbaye@univ-zig.sn

Received: 11 October 2019; Accepted: 7 November 2019; Published: 15 November 2019



Abstract: This study assesses the changes in precipitation (P) and in evapotranspiration (ET) under 1.5 °C and 2.0 °C global warming levels (GWLs) over Senegal in West Africa. A set of twenty Regional Climate Model (RCM) simulations within the Coordinated Regional Downscaling Experiment (CORDEX) following the Representative Concentration Pathways (RCP) 4.5 emission scenario is used. Annual and seasonal changes are computed between climate simulations under 1.5 °C and 2.0 °C warming, with respect to 0.5 °C warming, compared to pre-industrial levels. The results show that annual precipitation is likely to decrease under both magnitudes of warming; this decrease is also found during the main rainy season (July, August, September) only and is more pronounced under 2 °C warming. All reference evapotranspiration calculations, from Penman, Hamon, and Hargreaves formulations, show an increase in the future under the two GWLs, except annual Penman evapotranspiration under the 1.5 °C warming scenario. Furthermore, seasonal and annual water balances (P-ET) generally exhibit a water deficit. This water deficit (up to 180 mm) is more substantial with Penman and Hamon under 2 °C. In addition, analyses of changes in extreme precipitation reveal an increase in dry spells and a decrease in the number of wet days. However, Senegal may face a slight increase in very wet days (95th percentile), extremely wet days (99th), and rainfall intensity in the coming decades. Therefore, in the future, Senegal may experience a decline in precipitation, an increase of evapotranspiration, and a slight increase in heavy rainfall. Such changes could have serious consequences (e.g., drought, flood, etc.) for socioeconomic activities. Thus, strong governmental politics are needed to restrict the global mean temperature to avoid irreversible negative climate change impacts over the country. The findings of this study have contributed to a better understanding of local patterns of the Senegal hydroclimate under the two considered global warming scenarios.

Keywords: 1.5 °C and 2.0 °C global warming; water balance components; Senegal; CORDEX

1. Introduction

Climate change is considered one of the main challenges for social, economic, and environmental issues in Sub-Saharan Africa. These issues were underlined in the latest report of the Intergovernmental Panel on Climate Change [1], and they are likely to become more significant in the future. Recent studies over this region [2–6] have shown increased temperatures and decreased precipitation in the coming decades. Sylla al. [7] found heat stress issues such as cramp, heat exhaustion, and heat stroke in future climate scenarios. Furthermore, Weber et al. [8] found an increase in hot nights and longer and more frequent heat waves, while a decrease of wet spells and an increase of dry days were

found by Reference [9]. Additionally, risk of catastrophic floods and crop water stress are projected to increase, and the irrigation requirement might become frequent [10]. Such findings have shown how the West African region is vulnerable to climate change. In order to limit global warming, the international community came to the Paris Agreement in 2015. The key outcome of this agreement is to limit the increase of the global mean temperature below 2 °C, and ideally at 1.5 °C. Thereby, Senegal (West Africa) is committed to following the recommendations of the twenty-first session of the Conference of the Parties (COP 21) in Paris. The population in West Africa will face unprecedented heat discomfort even in the case of the Paris global warming scenario targets [7]. Senegal's economy is based primarily on agriculture, particularly the production of peanuts and cotton, but this sector has been hurt by drought and low commodity prices. A rapidly growing population is placing enormous stress on Senegal's limited land resources, agricultural production, and water resources. Over 80 percent of the population lives in the western half of the country; nearly 70 percent are farmers, but the urban population is steadily increasing [11]. Then, it becomes fundamental to investigate to what extent these warming targets will impact the hydroclimatology of the country, in order to guide decision making at local level. In this study, we thus aim to assess the impacts of 1.5 °C and 2.0 °C global warming levels (GWLs) on mean precipitation, potential evapotranspiration, simplified water balance, and extreme precipitation changes over Senegal; where, so far, no study has addressed the magnitude and the direction of hydroclimatic changes under these two warming scenarios (to the best of our knowledge). Precipitation and evapotranspiration are the key hydroclimatic variables of the water balance components that affect water resource availability in soil, surface water bodies, and vegetation. According to Reference [12], in humid regions, evapotranspiration is responsible for approximately 50% of the annual rainfall, whereas in arid regions, the proportion reaches 90%. Thus, the assessment of their changes is necessary for better water resource planning strategies. To achieve this work, twenty regional climate simulations from the Coordinated Regional Climate Downscaling Experiment (CORDEX, [13]) were used. CORDEX data (sea level pressure, surface temperature, and precipitation, etc.) have been successfully evaluated over West Africa [14–16].

This paper is structured as follows: After this introduction, materials and methods are described in Section 2. Subsequently, results and discussion are presented in Section 3. Finally, conclusion is provided in Section 4.

2. Materials and Methods

2.1. Study Area: Senegal Country

The study is focused over Senegal, located in West Africa (Figure 1). Senegal is the westernmost country on the African mainland and its capital (Dakar) has historically served as the gateway to West Africa. Senegal is a country bordered by Mauritania in the north, Mali to the east, Guinea to the southeast, and Guinea-Bissau to the southwest. Two distinct seasons characterize Senegal's climate, as follows: A dry season from roughly October to May and a rainy season from June to September. The mean annual rainfall from 1950 to 2010 was 600 mm; with a maximum of 1300 mm in the south, and a minimum of 300 mm in the north (Figure 1). Senegal has a wide range of bioclimatic regions, as follows: (i) The semiarid Sahel in the north is home to pastoral societies, (ii) the Sudanian region in the central and southern part of the country has a mix of settled farming communities and wooded savannas, and (iii) the sub-Guinean region of the southwest (particularly in Casamance or in Ziguinchor), where there are peoples who grow and produce a lot of rice, and live and exploit forest mangrove-fringed estuaries [11].

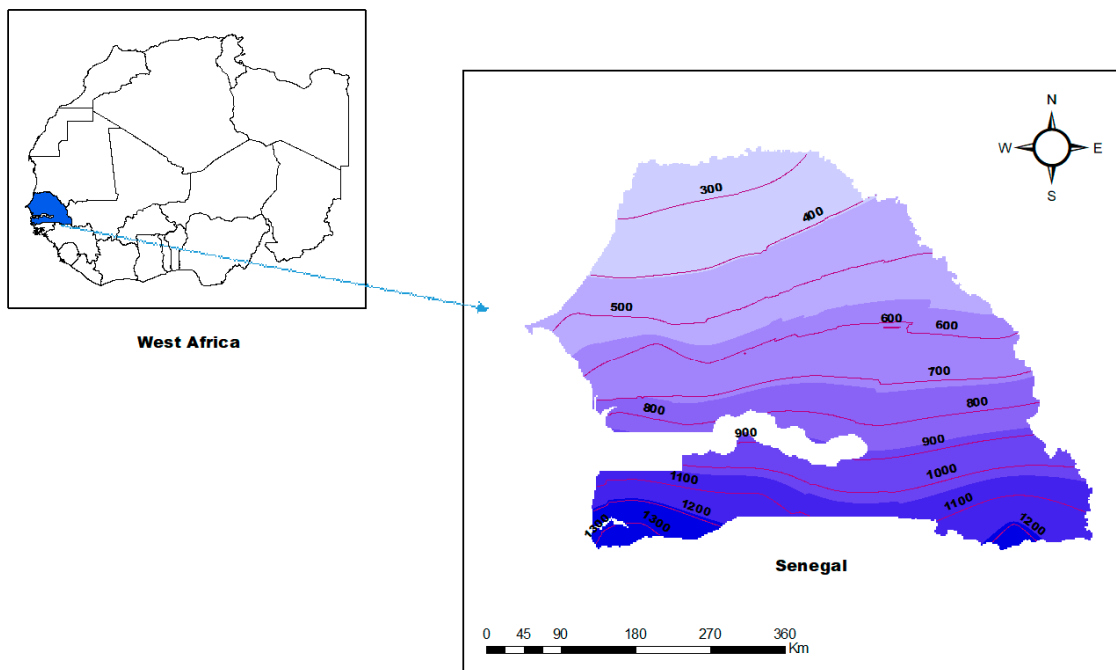


Figure 1. Senegal country (blue) in West Africa. Red lines are isohyets and numbers are their corresponding values in mm.

2.2. Data

In this study, daily observed rainfall (1950–2010) from the National Agency of Civil Aviation and Meteorology of Senegal (ANACIM) were used to generate the isohyets in Figure 1. We have also used precipitation and reference evapotranspiration from 20 regional climate simulations (see details in Table 1) within the Coordinated Regional Climate Downscaling Experiment (CORDEX, [13]). One of the goals of CORDEX is to provide regional climate simulations in order to better understand relevant regional/local climate phenomena, their variability, and changes, through downscaling.

Table 1. Climate model data with the name of the driving global climate model (GCM), institute, regional climate model (RCM), and the different periods of simulations. The reference period is the historical period obtained with 0.5 °C warming, with respect to the preindustrial in the same way as both targets (1.5 °C and 2 °C) in the future.

Driving GCM.	Institute	RCM	Reference Period	1.5 °C Warming Period	2.0 °C Warming Period
NCC-NorESM1-M	SMHI	RCA4	1976–2005	2029–2058	2064–2093
	DMI	HIRHAM5	1976–2005	2029–2058	2064–2093
	BCCR	WRF	1976–2005	2029–2058	2064–2093
MPI-M-MPI-ESM-LR	UQAM	CRCM5	1958–1987	2006–2035	2031–2060
	MPI	REMO	1958–1987	2006–2035	2031–2060
	SMHI	RCA4	1958–1987	2006–2035	2031–2060
	CLMcom	CCLM4–8–17	1958–1987	2006–2035	2031–2060
MOHC-HadGEM2-ES	SMHI	RCA4	1984–2005	2017–2046	2032–2061
	KNMI	RACMO22T	1984–2005	2017–2046	2032–2061
	CLMcom	CCLM4–8–17	1984–2005	2017–2046	2032–2061
ICHEC-EC-EARTH	SMHI	RCA4	1958–1987	2008–2037	2030–2059
	MPI	REMO	1958–1987	2008–2037	2030–2059
	KNMI	RACMO22T	1958–1987	2008–2037	2030–2059
	DMI	HIRHAM5	1958–1987	2008–2037	2030–2059
	CLMcom	CCLM4–8–17	1958–1987	2008–2037	2030–2059
CNRM-CERFACS-CNRM-CM5	SMHI	RCA4	1974–2003	2021–2050	2043–2072
	CLMcom	CCLM4–8–17	1974–2003	2021–2050	2043–2072

Table 1. Cont.

Driving GCM.	Institute	RCM	Reference Period	1.5 °C Warming Period	2.0 °C Warming Period
CCCma-CanESM2	UQAM	CRCM5	1969–1998	2006–2035	2018–2047
	SMHI	RCA4	1969–1998	2006–2035	2018–2047
	CCCma	CanRCM4	1969–1998	2006–2035	2018–2047

Note: NCC-NorESM1-M: Norwegian Climate Centre, Norwegian Earth System Model 1—Medium Resolution; MPI-M-ESM-LR: Max Planck Institute for Meteorology—Earth System Model Low Resolution; MOHC-HadGEM2-ES: Met Office Hadley Centre—Earth System Model; ICHEC-EC-EARTH: Irish Centre for High-End Computing Earth System Models; CNRM-CERFACS-CNRM-CM5: Centre National de Recherches Météorologiques—Centre Européen de Recherche et de Formation Avancée en Calcul Scientifique; CCCma-CanESM2: Canadian Center for Climate Modelling and Analysis; SMHI: Swedish Meteorological and Hydrological Institute; DMI: Danish Meteorological Institute; BCCR: Bjerknes Centre for Climate Research ;RCA: Rossby Centre regional Atmospheric climate model;WFR: Weather Research and Forecasting; HIRHAM: regional atmospheric climate model (RCM) based on a subset of the HIRLAM (High Resolution Limited Area Model) and ECHAM ((Acronym of ECMWF(European Centre for Medium-Range Weather Forecasts.) and Hamburg) models; UQAM: Université du Québec à Montréal; CRCM: Coupled atmosphere-ocean Regional Climate Model; REMO: Regional Climate Model; CLMcom: Climate Limited-area Modelling Community; CCLM: COSMO-CLM Regional Climate Model; RACMO: Regional Atmospheric Climate Model; KNMI: Royal Dutch Meteorological Institute.

These simulations are generated by eight Regional Climate Models (RCMs) driven by six Global Climate Models (GCMs). These data are on half degree ($0.5^\circ \times 0.5^\circ$) horizontal resolution, and at daily time step. Note that the RCMs driven by the same GCM have the same reference period and the same future warming periods. Simulations based on RCP4.5 under 1.5 °C and 2.0 °C global warming are in line with the Paris Agreement. These warming levels are generated compared to the pre-industrial period; details on the methodology to derive the warming scenarios are given in Reference [7].

2.3. Methods

Precipitation and reference or potential evapotranspiration are analyzed on seasonal (July, August, September (JAS); October, November, December (OND); January, February, March (JFM); and April, May, June (AMJ)) and annual time scales; but here we focus on the JAS rainy season in our analyses. This latter season corresponds to the main rainy season in Senegal. Most extreme meteorological phenomena occur during this period of rainfall. The simulated reference evapotranspiration is estimated following the Penman–Monteith method, as recommended by the Food and Agriculture Organization (FAO) [17–19]. In the following, Penman refers to Penman–Monteith, and Hargreaves refers to Hargreaves and Samani.

The Penman–Monteith reference evapotranspiration according to the FAO56 equation is given by the following:

$$ET0 = \frac{0.408\Delta(R_n - G) + \gamma \frac{900}{T+273} U_2 (e_s - e_a)}{\Delta + \gamma(1 + 0.34U_2)}, \quad (1)$$

where $ET0$ is the potential evapotranspiration (mm day^{-1}), R_n is the net irradiance ($\text{MJm}^{-2} \text{day}^{-1}$), G is the soil heat flux density ($\text{MJm}^{-2} \text{day}^{-1}$), e_s is the saturation vapor pressure (kPa), e_a is the actual vapor pressure (kPa), $e_s - e_a$ is the saturation vapor pressure deficit (kPa), Δ is the slope vapor pressure curve ($\text{kPa } ^\circ\text{C}^{-1}$), γ is the psychrometric constant ($\text{kPa } ^\circ\text{C}^{-1}$), T is the mean air temperature at 2 m height ($^\circ\text{C}$), and U_2 is the wind speed at 2 m height (m s^{-1})

The Hamon (1961) potential evapotranspiration is as follows:

$$ET0 = 0.55 \left(\frac{N}{12} \right)^2 \left(\frac{4.95 e^{0.062 T_{mean}}}{100} \right) 25.4, \quad (2)$$

where, $ET0$ (mm day^{-1}) is the potential evapotranspiration, N is the theoretical maximum daily insolation (hours), and T_{mean} is the average of temperatures ($^\circ\text{C}$).

The Hargreaves evapotranspiration according to FAO56 is given by the following:

$$ET_0 = 0.0023(T_{mean} + 17.8)(T_{max} - T_{min})^{0.5}R_a, \quad (3)$$

where ET_0 is the reference evapotranspiration, R_a is the extra-terrestrial radiation (mm day^{-1}), for a given latitude and day (R_a ($\text{MJm}^{-2} \text{ day}^{-1}$) is obtained from tables or calculated), T_{max} is the daily maximum temperature ($^{\circ}\text{C}$), and T_{min} is the daily minimum temperature ($^{\circ}\text{C}$).

All the analyses are done by taking the ensemble mean of all regional climate model simulations. The changes are obtained by the difference between the future warming periods minus the reference period (historical period). The water balance is defined as the difference between precipitation and evapotranspiration (P-PET). In addition, we computed climate extreme indices, such as the maximum number of consecutive dry days (CDD), the maximum number of consecutive wet days (CWD), the 95th percentile for very wet days, the 99th percentile for extremely wet days, and the simple rainfall intensity index (SDII). Some details of these indices are given in Table 2. As in lot of climate change studies [16,20,21], a threshold of 1 mm is taken for wet days. Furthermore, annual cycles of precipitation, evapotranspiration, and water balance, are calculated. We use the Student's t -test (confidence level of 95%) to highlight the significance of changes.

Table 2. Climate indices.

Index Name	Index Signification	Unit
Simple daily rainfall intensity index (SDII)	Let PR_{wj} be the daily precipitation amount on wet days, $PR \geq 1$ mm in period j . If W represents the number of wet days in j , then: $SDII_j = (\sum_{w=1}^W PR_{wj}) / W$	mm
Maximum number of consecutive dry days (CDD)	Let PR_{ij} be the daily precipitation amount on day i in period j . Count the largest number of consecutive days where $PR_{ij} < 1$ mm	day
Maximum number of consecutive wet days (CWD)	Let PR_{ij} be the daily precipitation amount on day i in period j . Count the largest number of consecutive days where $PR_{ij} > 1$ mm	day
Very wet days (95P)	95th percentile of precipitation on wet days means the value above which 5% of the daily precipitation events are found.	mm
Extremely wet days (99P)	99th percentile of precipitation on wet days means the value above which 1% of the daily precipitation events are found.	mm

3. Results and Discussion

3.1. Annual and Seasonal Changes of Precipitation and Evapotranspiration

Overall, annual precipitation is likely to decrease in the whole country (Figure 2) under the two GWLs. This decrease is more pronounced from southwest to northwest with the 2.0°C warming scenario (up to 60 mm). Precipitation changes are significant in the whole country, except the southeast region where no significant changes were found.

This decline of precipitation may be due to a decrease of moisture supply from the southwest Atlantic Ocean; because as sea surface temperatures (SSTs) are likely to increase due global warming, this will reduce the thermal gradient between ocean and land and thus decrease the northward extent of the monsoon [22].

For the reference evapotranspiration, a general increase is projected according to Hamon and Penman formulations for the two scenarios; however, a small decrease (not significant) is noted under 1.5°C global warming with Hargreaves estimation. This latter estimate also depicts the smallest increase under the strongest global warming scenario (2.0°C). Hamon evapotranspiration changes are the largest (more than 160 mm), followed by Penman and Hargreaves, respectively. The particularity of Hargreaves estimates may be explained by the different contributions of the different seasons (Figure S2 in the supplementary materials) in the annual mean (Figure 2).

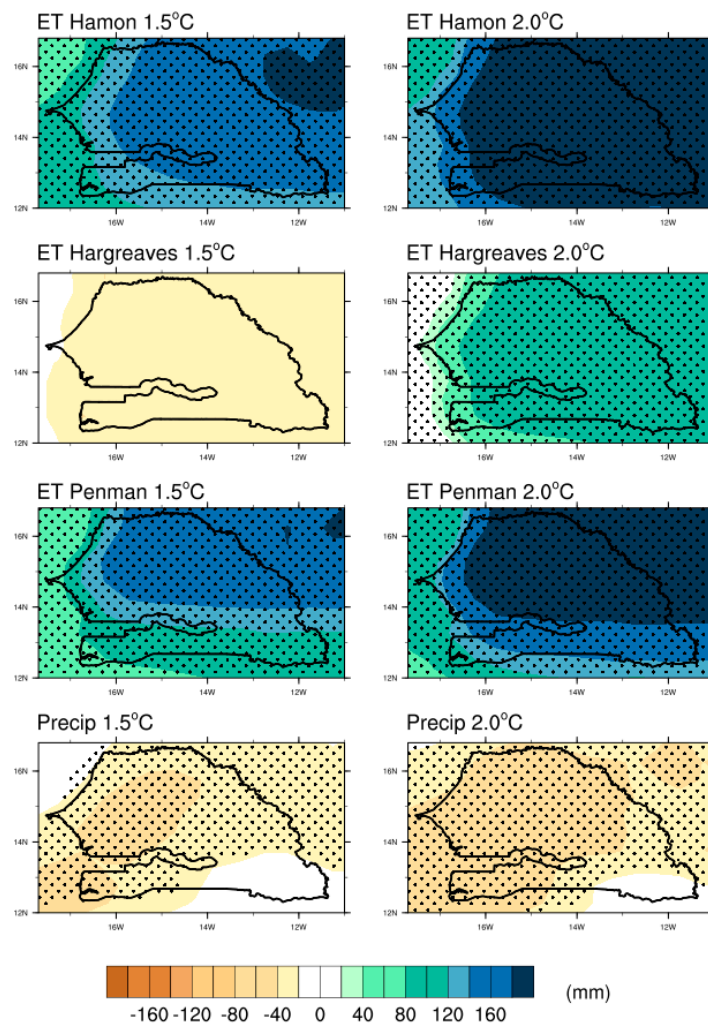


Figure 2. Annual evapotranspiration (ET, first row: Hamon, second row: Hargreaves, third row: Penman) and precipitation (Precip, fourth row) changes under 1.5 °C (left column) and 2 °C (right column) GWLs. Statistically significant changes (Student's *t*-test) at 95% confidence level are represented by black dots.

In all seasons (JFM, AMJ, JAS, and OND), both Penman and Hamon estimates show increased evapotranspiration, while only two seasons (JAS and OND) show an increase of evapotranspiration with Hargreaves (Figures S1–S3). This suggests that annual changes are more influenced by changes during the long dry season. In the dry season, the ET is more influenced by the amount of moisture stored in the soil during the previous rainy season than by rainfall events during the dry season [23]. Furthermore, as found by Reference [6], minimum temperatures increase faster than maximum temperatures; thus, the temperature gradients ($T_{max} - T_{min}$) used in Hargreaves may decrease and consequently impact the ET estimates. The northeast of Senegal depicts the greatest increase of potential evapotranspiration (Figure 2). The differences in ET estimates are mainly due to the different variables and the coefficients used by authors to estimate evapotranspiration. The radiations are responsible for the highest values of evapotranspiration due to the available energy, which changes large quantities of liquid water into water vapor. The surface radiation balance is one the main factor responsible for the evapotranspiration process, as highlighted in Ferreira et al. [24]. In the main rainy season (JAS), precipitation is projected to decrease in the whole country, except in the southeast where a slight increase (0.1 mm) is found (Figure 3). The localities situated in the north, northeast, center, and southwest could face the most severe decline of rainfall (0.4 mm). This decline is significant at a 5% significance level.

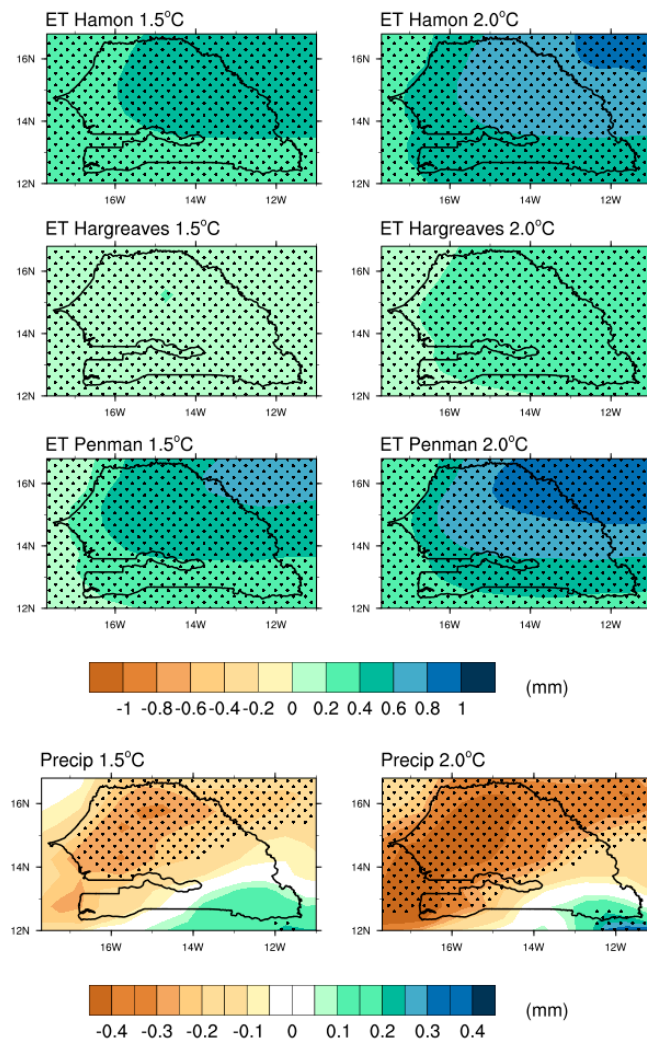


Figure 3. Seasonal evapotranspiration (ET, first row: Hamon, second row: Hargreaves, third row: Penman) and precipitation (Precip, fourth row) changes under 1.5 °C (**left column**) and 2 °C (**right column**) GWLs. Statistically significant changes (Student's *t*-test) at 95% confidence level are represented by black dots.

These differences between the north and the southeast can be explained by the strong land surface heterogeneities, the topography, and the remote response of local precipitation to changes in vegetation dynamics [25,26].

This increase of rainfall in the southwest part may also be caused by thermodynamic changes in moisture content and local/mesoscale feedbacks, rather than change in the general circulation [8]. Furthermore, the increase in the seasonal mean of precipitation may be linked to the contribution of the potential increase of extremely wet days, even though there will be a lower number of rainy days. All estimates of reference evapotranspiration show an increase in the whole country under both warming scenarios. In these seasonal estimates, greater changes are expected with Penman evapotranspiration, followed by Hamon and Hargreaves evapotranspiration, respectively. The center and the northeast of Senegal would experience the most substantial increase of evapotranspiration in the coming decades.

3.2. Annual and Seasonal Changes of the Water Balance (*P-ET*)

The annual water balance is represented in Figure 4. A general water deficit can be seen (more than 180 mm), which means that the water losses through the process of evapotranspiration are greater than

the incoming water from precipitation in the water budget. Hamon and Penman evapotranspiration estimates show the highest water stress.

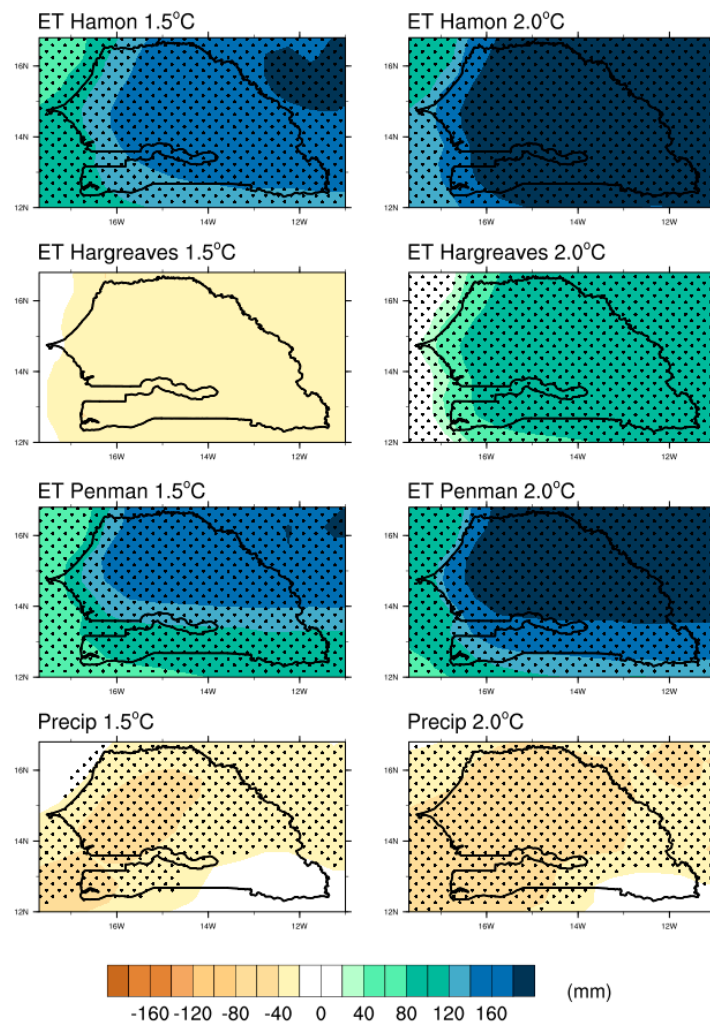


Figure 4. Annual water balance (Pr minus ET, first row: Hamon, second row: Hargreaves, third row: Penman) changes under 1.5 °C (left column) and 2.0 °C (right column) GWLs. Statistically significant changes (Student's *t*-test) at 95% confidence level are represented by black dots.

However, Hargreaves evapotranspiration estimates under 1.5 °C warming to show no significant changes of water shortage in the majority of the country; except the southeast, which shows possible wet conditions. The changes with Hargreaves under the 1.5 °C scenario are not important (around zero), and those under the 2.0 °C scenario are very low compared to the other estimates. The localities with high evapotranspiration and less precipitation will become drier (e.g., northern Senegal). Moreover, in this semi-arid region where dry and hot weather conditions prevail during the long dry season, the wind speed intensifies the evaporation process. This annual water decline is seen also in the seasonal change (JAS) of the water balance in Figure 5. These conditions are also generally found in the other seasons (Figures S4–S6).

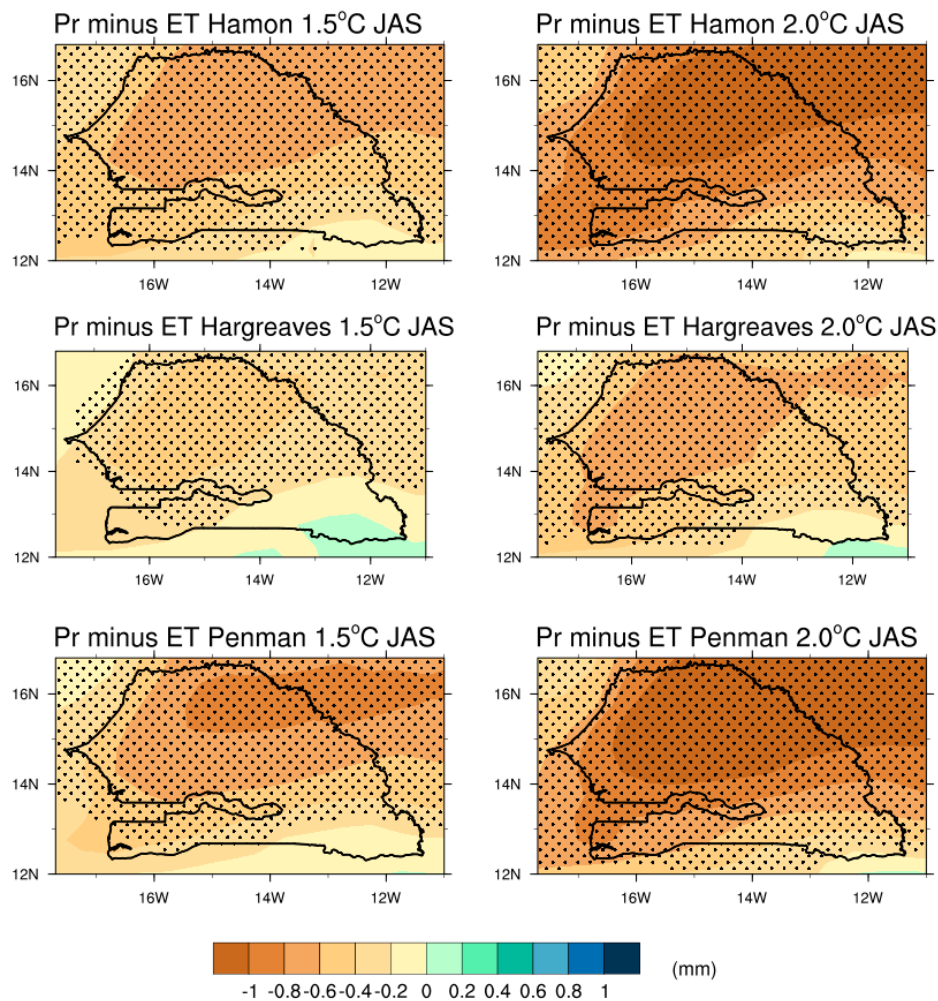


Figure 5. Seasonal water balance (Pr minus ET, first row: Hamon, second row: Hargreaves, third row: Penman) changes under 1.5 °C (left column) and 2.0 °C (right column) GWLs. Statistically significant changes (Student's *t*-test) at 95% confidence level are represented by black dots.

The decrease of water is general in the whole country, along with significant changes in the center and the northeast parts of the country under both GWLs. Evapotranspiration estimates from Hamon and Penman show the most drastic decrease of available water. This means that Senegal could experience drier conditions in the future, and this will seriously affect socioeconomic activities relying upon water resources. The increase of evapotranspiration combined with the decrease of precipitation would cause hydrological drought conditions with evidence of low water supplies. In addition, the fact that we have water stress during the main rainy season (JAS) may be due to an overestimation of potential evapotranspiration with all estimates. ET estimates use parameters such as temperatures, radiations, winds, humidity, etc., depending of the formula used. An overestimation of these variables by climate models will affect the potential evapotranspiration. Most of climate models overestimate the response to increasing greenhouse gases and other anthropogenic forcing [27].

The lowest increase of evapotranspiration in the southeast part of Senegal is related to the abundance of humidity in the air that diminishes atmospheric water demand, notwithstanding the energy input [28]. In such conditions, the considerable amount of water vapor in the atmosphere (closer to saturation) is responsible for the fact that less additional water can be stored; hence, the evapotranspiration rate is low [28].

On the contrary, northern Senegal (hot and dry region) absorbs large amounts of water due to the presence of substantial energy and the atmospheric desiccating power. This enhances the water holding capacity of the atmosphere and therefore increases the evapotranspiration rate.

3.3. Seasonal Changes of Extreme Precipitation

In this section, we present the potential changes of extreme precipitation over Senegal during the rainy season (JAS). An increase in the maximum number of consecutive dry days (up to 16 days) in the whole country is projected under both GWLs (Figure 6). The northern part of the country is significantly likely to experience the driest conditions in the future under 2.0 °C global warming.

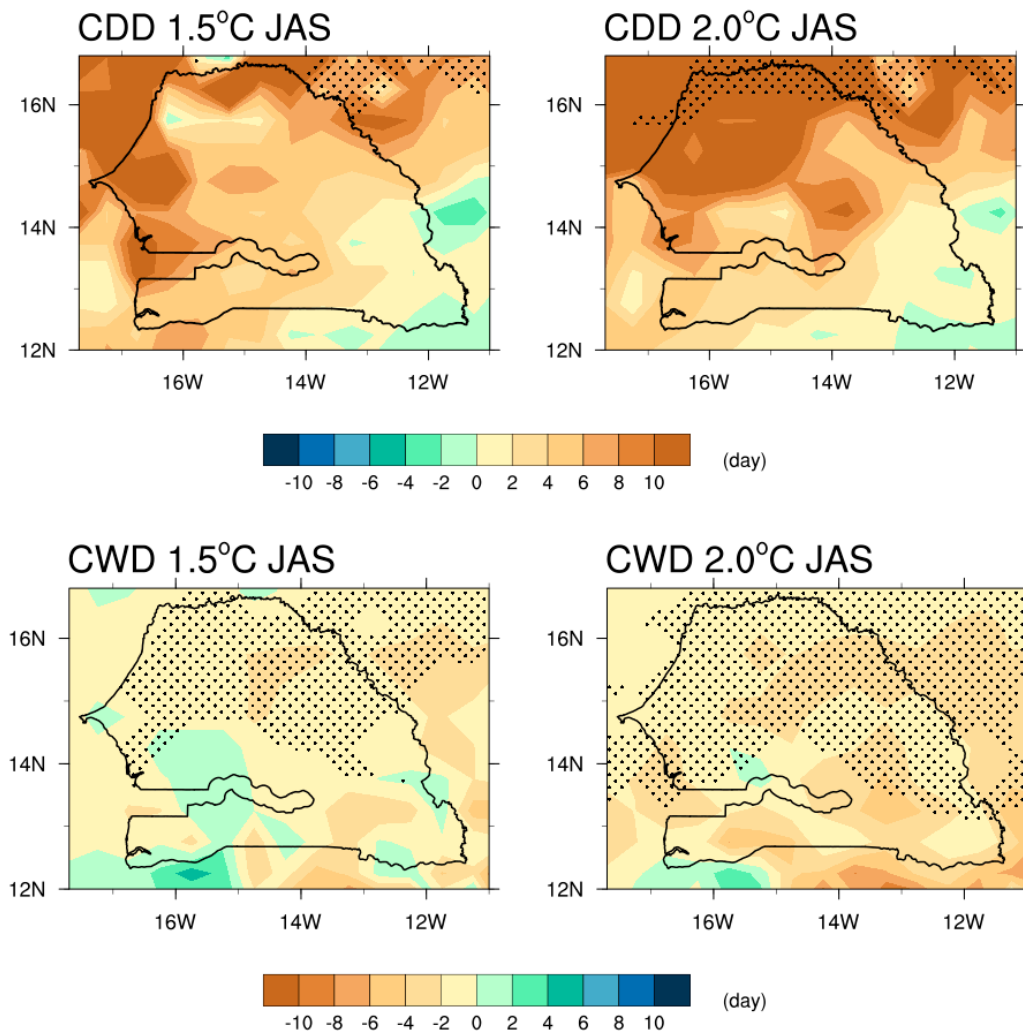


Figure 6. Maximum number of consecutive dry days (CDD) (**first row**) and maximum number of consecutive wet days (CWD) (**second row**) changes under 1.5 °C (**left column**) and 2.0 °C (**right column**) GWLs. Statistically significant changes (Student's *t*-test) at 95% confidence level are represented by black dots.

However, in the south and the southwest zones, a GWL of 1.5 °C shows the highest increase of dry spells. In western Sahel, a significant increase in the length of dry spells and a decrease in the standardized precipitation evapotranspiration index was found by Reference [29].

These drier conditions can be attributed to the considerable decrease of the number of wet days, as shown in the second row of Figure 6; even though a few localities could benefit from a slight increase of wet days. These results are in phase with the general decrease of annual and seasonal (JAS) precipitation.

The alternation of dry and wet periods during the rainy season will contribute to increase the vulnerability of food production [10]. Furthermore, these projected changes may have significant consequences on fragile ecosystems and agriculture, as they are strongly affected by the length of wet and dry periods [30]. However, in the future, extremely wet days could slightly increase under both warming scenarios, as shown in Figure 7. The southeast of the country exhibits the most substantial and significant increase of extreme precipitation (up to 12 mm).

Considering the 95th percentile of wet days, the increase of very wet days seems to be relatively more important under 1.5 °C than under 2.0 °C (Figure 7). This response is almost the opposite with the 99th percentile of extremely wet days.

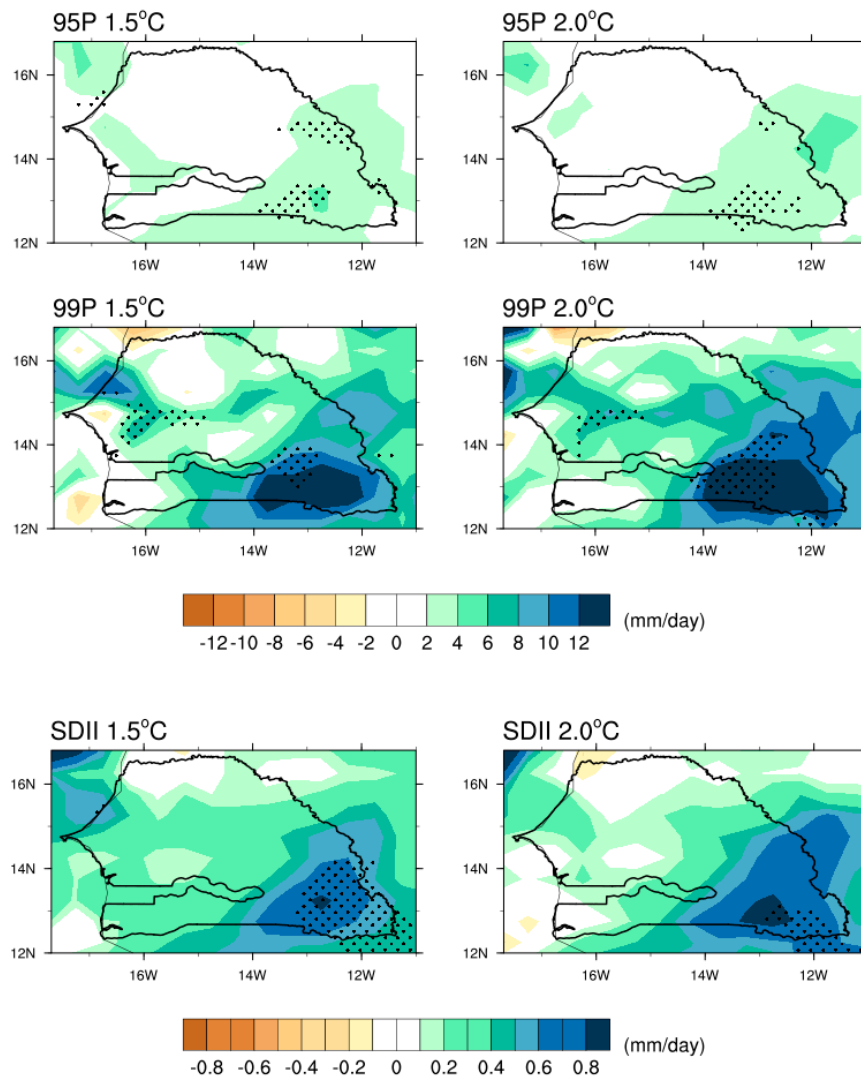


Figure 7. Seasonal (JAS) changes of very wet days (95P) (**first row**), extremely wet days (99P) (**second row**), and rainfall intensity index (SDII) (**third row**) changes under 1.5 °C (**left column**) and 2.0 °C (**right column**) GWLs. Statistically significant changes (Student's *t*-test) at 95% confidence level are represented by black dots.

In general, the most intense precipitation prevails in the southeast part of the country (Figure 7). This increase of very heavy precipitation could be the result of an intensification of the hydrological cycle under warming conditions through the process of Clausius–Clapeyron [31]. With this probable increase of extreme rainfall, this part of the country could experience risk of flooding events in the future under global warming conditions.

Our results show that changes in extreme events are likely to be more substantial under the 2.0 °C global warming scenario. Then, efforts and politics that promote to limit warming to 1.5 °C will have significant benefits in terms of reducing the potential impacts of these extremes [32].

3.4. Seasonal Cycle of Evapotranspiration, Precipitation, and the Water Balance (P-ET)

Changes of the seasonal cycle of precipitation, potential evapotranspiration, and water balance are presented in Figure 8. It is clearly noted that, generally, potential evapotranspiration will increase under both warming scenarios, with the highest increase with Penman (Figure 8a) and Hamon (Figure 8c) estimates under the 2.0 °C scenario. ET depends on several factors such as wind, temperature, humidity, water availability, radiation, etc. For example the well-known increase of temperature and radiation, will in turn increase the rate of evaporation because of the conversion of liquid water to water vapor by the available energy.

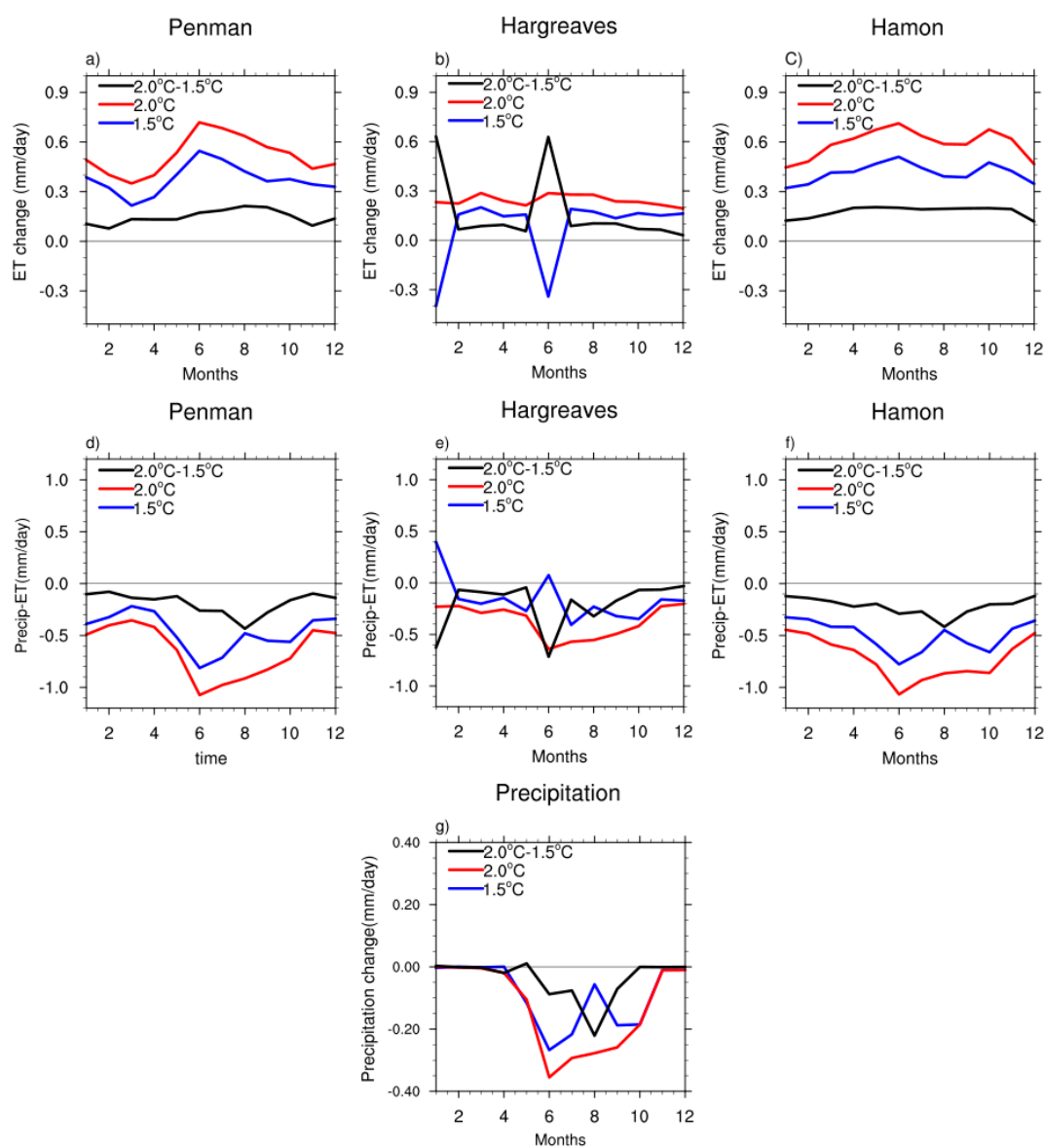


Figure 8. Seasonal cycle of Evapotranspiration (a,d: Penman, Hargreaves, and Hamon), water balance (P-ET) (b,e,g: with Penman, Hargreaves, and Hamon) and Precipitation changes (c,f) under 1.5 °C and 2.0 °C GWLs.

For Hargreaves (Figure 8b), we abnormally found a slight decrease of potential evapotranspiration in January and June. This situation may be explained by the fact that Hargreaves estimate is a temperature-based method, the decline of evapotranspiration with the lowest scenario during the main rainy season can be due to a diminished effect of mean temperature triggered by short-wave radiation [33].

Furthermore, precipitation is projected to decrease in all months under both global warming levels (Figure 8g); this situation is more amplified under the 2.0 °C warming scenario. As for the water balance, a general water deficit is found in the whole seasonal cycle (Figure 8d–f). This can be justified by a combination of a decrease in precipitation and an increase in potential evapotranspiration.

Table 3 summarizes the annual mean over the whole country for precipitation, potential evapotranspiration, and water balance at 5% significance level. As shown in the above results, precipitation and water balance could decrease in the future under both GWLs [34]. Moreover, potential evapotranspiration is projected to considerably increase for all estimates and warming scenarios, except with Hargreaves, which depicts a decrease under 1.5 °C warming. This decrease is not significant.

From these findings, it is obvious that Senegal will face drier conditions even with the global warming targets of the Paris Agreement in 2015. Socioeconomic activities such as agriculture, livestock, fishing, etc., will be seriously affected.

Table 3. Annual mean changes of precipitation, evapotranspiration, and water balance and the corresponding *p* values at 5% significance level. Bold *p* values indicate no significant changes.

Variables (mm)	1.5 °C	<i>p</i> Value	2.0 °C	<i>p</i> Value
Precipitation	−32.28	0.0085	−46.52	0.0035
ET_Hamon	150.27	1.1545×10^{-21}	215.29	6.9203×10^{-32}
ET_Hargreaves	−27.62	0.7085	88.63	5.6167×10^{-11}
ET_Penman	136.19	8.9017×10^{-15}	189.58	6.6405×10^{-20}
P-ET_Hamon	−182.55	0.000168	−261.81	5.8164×10^{-7}
P-ET_Hargreaves	−4.66	0.48960	−135.16	0.00064
P-ET_Penman	−168.47	0.00084	−236.11	0.00036

4. Conclusions

The assessment of the impacts of 1.5 °C and 2.0 °C global warming scenarios over Senegal was done in this study. Precipitation, potential evapotranspiration, water balance, and extreme precipitation were analyzed using 20 RCM simulations of the Coordinated Regional Climate Downscaling Experiment (CORDEX), Africa.

The results show that Senegal is likely to face a considerable decrease of the annual and seasonal mean of precipitation under both warming scenarios. However, potential evapotranspiration is projected to generally increase with Hamon, Penman, and Hargreaves estimates, and this will amplify water losses from soil, water bodies, and plants. Furthermore, the estimation of the water balance has revealed substantial water deficit in the future under the two warming scenarios. With regards to these findings, it is clear that climate change will considerably affect water balance components in Senegal under the two GWLs of the Paris Agreement towards in the future. Drier conditions are expected, particularly in the northern part of the country. This means that the socioeconomic activities which depend on water resources (e.g., agriculture) will be negatively affected. Farmers should use crops resistant to heat and water stress. Moreover, water saving technologies could also be promoted and developed to reduce the consequences of water shortage.

The analysis of extreme precipitation has revealed that even though the annual and seasonal mean of precipitation is projected to decrease, heavy and extremely wet days, and intense rainfall, will increase. It is interesting to note that the southeast part of Senegal is likely to face more of these extremes, and presents the highest risk of flooding events. However, on the other hand, considerable

dry spells could occur during the rainy season. In all analyses, changes under the 2.0 °C scenario are more substantial and significant than changes under 1.5 °C global warming.

Finally, our results suggest that under the warming targets of the Paris Agreements, local changes could have consequences that are likely to be above those of the global mean temperature changes. The provided information on the potential consequences of these warming scenarios might help decision makers to reorient their planning strategies in the context of a changing climate. This study should be extended to the entirety of the sub-Saharan countries in order to help them develop sustainable adaptation strategies and reduce their vulnerability to climate change.

Supplementary Materials: The following are available online at <http://www.mdpi.com/2073-4433/10/11/712/s1>, Figure S1: Seasonal Hamon Evapotranspiration changes (first row: April-May-June [AMJ], second row: July-August-September [JAS], third row: October-November-December [OND], fourth row: January-February-March [JFM]) under 1.5 °C (left column) and 2 °C (right column) GWLs, Figure S2: Seasonal Hargreaves Evapotranspiration changes (first row: April-May-June [AMJ], second row: July-August-September [JAS], third row: October-November-December [OND], fourth row: January-February-March [JFM]) under 1.5 °C (left column) and 2 °C (right column), Figure S3: Seasonal Penman Evapotranspiration changes (first row: April-May-June [AMJ], second row: July-August-September [JAS], third row: October-November-December [OND], fourth row: January-February-March [JFM]) under 1.5 °C (left column) and 2 °C (right column) GWLs, Figure S4: Seasonal water balance (Pr-ET, first row: Hamon, second row: Hargreaves, third row: Penman) changes under 1.5 °C (left column) and 2 °C (middle column) GWLs, and The column on the right provides the difference between 2.0 °C and 1.5 °C GWLs, Figure S5: Seasonal water balance (Pr-ET, first row: Hamon, second row: Hargreaves, third row: Penman) changes under 1.5 °C (left column) and 2 °C (middle column) GWLs, and The column on the right provides the difference between 2.0 °C and 1.5 °C GWLs, Figure S6: Seasonal water balance (Pr-ET, first row: Hamon, second row: Hargreaves, third row: Penman) changes under 1.5 °C (left column) and 2 °C (middle column) GWLs, and The column on the right provides the difference between 2.0 °C and 1.5 °C GWLs.

Author Contributions: M.L.M. and M.B.S. conceived and designed the experiments. M.B.S. generated the climate simulations data and gave suggestions for the analysis; M.L.M. and M.T. performed the data analysis and wrote the paper.

Funding: This research received no external funding.

Acknowledgments: The authors thank the Laboratoire d’Océanographie, des Sciences de l’Environnement et du Climat (LOSEC) of the University of Assane Seck, Ziguinchor where the work has been mainly done, and the WASCAL Competence where the climate models data have been generated. The editor and the anonymous reviewers are also sincerely thanked for their valuable comments and suggestions to improve the quality of the paper.

Conflicts of Interest: The authors declare no conflict of interest.

References

1. IPCC. *Climate Change 2014: Synthesis Report. Contribution of Working Groups I, II and III to the Fifth Assessment Report of the Intergovernmental Panel on Climate Change*; Core Writing Team, Pachauri, R.K., Meyer, L.A., Eds.; IPCC: Geneva, Switzerland, 2014; 151p.
2. Diallo, I.; Sylla, M.B.; Giorgi, F.; Gaye, A.T.; Camara, M. Multimodel GCM-RCM ensemble based projections of temperature and precipitation over West Africa for the early 21st century. *Int. J. Geophys.* **2012**, *12*, 972896. [[CrossRef](#)]
3. Mariotti, L.; Diallo, I.; Coppola, E.; Giorgi, F. Seasonal and intraseasonal changes of African monsoon climates in 21st century CORDEX projections. *Clim. Change* **2014**, *125*, 53–65. [[CrossRef](#)]
4. Mbaye, M.L.; Haensler, A.; Hagemann, S.; Gaye, A.T.; Moseley, C.; Afouda, A. Impact of statistical bias correction on the projected climate change signals of the regional climate model REMO over the Senegal River Basin. *Int. J. Climatol.* **2015**, *36*, 2035–2049. [[CrossRef](#)]
5. Tall, M.; Sylla, M.B.; Diallo, I.; Pal, J.S.; Faye, A.; Mbaye, M.L.; Gaye, A.T. Projected impact of climate change in the hydroclimatology of Senegal with a focus over the Lake Guiers for the twenty-first century. *Theor. Appl. Climatol.* **2016**, *129*, 655–665. [[CrossRef](#)]
6. Mbaye, M.L.; Diatta, S.; Gaye, A.T. Climate Change Signals Over Senegal River Basin Using Regional Climate Models of the CORDEX Africa Simulations. In *Proceedings of the Second International Conference, InterSol 2018*, Kigali, Rwanda, 24–25 March 2018.

7. Sylla, M.B.; Faye, A.; Giorgi, F.; Diedhiou, A.; Kunstmann, H. Projected heat stress under 1.5 °C and 2 °C global warming scenarios creates unprecedented discomfort for humans in West Africa. *Earth's Fut.* **2018**, *6*, 1029–1044. [[CrossRef](#)]
8. Weber, T.; Haensler, A.; Rechid, D.; Pfeifer, S.; Eggert, B.; Jacob, D. Analyzing regional climate change in Africa in a 1.5, 2, and 3 °C global warming world. *Earth's Fut.* **2018**, *6*, 643–655. [[CrossRef](#)]
9. Abiodun, B.J.; Adegoke, J.; Abatan, A.A.; Ibe, C.A.; Egbebiyi, T.S.; Engelbrecht, F.; Pinto, I. Potential impacts of climate change on extreme precipitation over four African coastal cities. *Clim. Change* **2017**, *143*, 399–413. [[CrossRef](#)]
10. Déqué, M.; Calmanti, S.; Christensen, O.B.; Dell Aquila, A.; Maule, C.F.; Haensler, A.; Nikulin, G.; Teichmann, C. A multi-model climate response over tropical Africa at +2 °C. *Clim. Serv.* **2017**, *7*, 87–95. [[CrossRef](#)]
11. Comité Permanent Inter-états de Lutte contre la Sécheresse dans le Sahel (CILSS). *Landscapes of West Africa—A Window on a Changing World*; CILSS: Ouagadougou, Burkina Faso, 2016; 219p.
12. Zhao, L.; Xia, J.; Xu, C.; Wang, Z.; Sobkowiak, L.; Long, C. Evapotranspiration estimation methods in hydrological models. *J. Geogr. Sci.* **2013**, *23*, 359–369. [[CrossRef](#)]
13. Giorgi, F.; Jones, C.; Asrar, G. Addressing climate information needs at the regional level: The CORDEX framework. *World Meteorol. Org. Bull.* **2009**, *58*, 175–183.
14. Dosio, A.; Panitz, H.J.; Schubert-Frisius, M.; Lüthi, D. Dynamical downscaling of CMIP5 global circulation models over CORDEX-Africa with COSMO-CLM: Evaluation over the present climate and analysis of the added value. *Clim. Dyn.* **2015**, *44*, 2637–2661. [[CrossRef](#)]
15. Klutse, N.A.B.; Sylla, M.B.; Diallo, I.; Sarr, A.; Dosio, A.; Diedhiou, A.; Kamga, A.; Lamptey, B.; Ali, A.; Gbobaniyi, E.O.; et al. Daily characteristics of West African summer monsoon precipitation in CORDEX simulations. *Theor. Appl. Climatol.* **2015**, *123*, 369–386. [[CrossRef](#)]
16. Nikiema, P.M.; Sylla, M.B.; Ogunjobi, K.; Kebe, I.; Gibba, P.; Giorgi, F. Multi-model CMIP5 and CORDEX simulations of historical summer temperature and precipitation variabilities over West Africa. *Int. J. Climatol.* **2017**, *37*, 2438–2450. [[CrossRef](#)]
17. Allen, R.G.; Pereira, L.S.; Raes, D.; Smith, M. *Crop Evapotranspiration—Guidelines for Computing Crop Water Requirements*; FAO Irrigation and Drainage Paper; UN Food and Agriculture Organization (FAO): Rome, Italy, 1998; Volume 56.
18. Hamon, W.R. Estimating potential evapotranspiration. *J. Hydraul. Eng. ASCE* **1961**, *87*, 107–120.
19. Hargreaves, G.; Samani, Z. Reference crop evapotranspiration from temperature. *Appl. Eng. Agric.* **1985**, *1*, 96–99. [[CrossRef](#)]
20. Sillmann, J.; Kharin, V.V.; Zwiers, F.W.; Zhang, X.; Bronaugh, D. Climate extremes indices in the CMIP5 multimodel ensemble: Part 2. Future climate projections. *J. Geophys. Res. Atmos.* **2013**, *118*, 2473–2493. [[CrossRef](#)]
21. Sylla, M.B.; Giorgi, F.; Pal, J.S.; Gibba, P.; Kebe, I.; Nikiema, M. Projected changes in the annual cycle of high-intensity precipitation events over West Africa for the late twenty-first century. *J. Clim.* **2015**, *28*, 6475–6488. [[CrossRef](#)]
22. Messenger, C.; Gallée, H.; Brasseur, O. Precipitation sensitivity to regional sst in a regional climate simulation during the west african monsoon for two dry years. *Clim. Dyn.* **2004**, *22*, 249–266. [[CrossRef](#)]
23. Silva, J.; Da Renato, O.; De Souza, E.B.; Tavares, A.L.; Mota, J.A.; Ferreira, D.B.S.; Souza-Filho, P.W.M.; Da Rocha, E.J.P. Three decades of reference evapotranspiration estimates for a tropical watershed in the eastern Amazon. *An. Acad. Bras. Ciênc* **2017**, *89*, 1985–2002. [[CrossRef](#)]
24. Ferreira, J.P.; Sousa, A.; Vitorino, M.; De Souza, E.; De Souza, P. Estimate of evapotranspiration in the eastern Amazon using SEBAL. *Rev. Cienc. Agrar.* **2013**, *56*, 33–39.
25. Sy, S.; Noblet-Ducoudré, N.D.; Quesada, B.; Sy, I.; Dieye, A.M.; Gaye, A.T.; Sultan, B. Land-Surface Characteristics and Climate in West Africa: Models' Biases and Impacts of Historical Anthropogenically-Induced Deforestation. *Sustainability* **2017**, *9*, 1917. [[CrossRef](#)]
26. Klein, C.; Bliefernicht, J.; Heinzeller, D.; Gessner, U.; Klein, I.; Kunstmann, H. Feedback of observed interannual vegetation change: A regional climate model analysis for the West African monsoon. *Clim. Dyn.* **2017**, *48*, 2837. [[CrossRef](#)]

27. Flato, G.; Marotzke, J.; Abiodun, B.; Braconnot, P.; Chou, S.C.; Collins, W.; Cox, P.; Driouech, F.; Emori, S.; Eyring, V.; et al. Evaluation of Climate Models. In *Climate Change: The Physical Science Basis. Contribution of Working Group I to the Fifth Assessment Report of the Intergovernmental Panel on Climate Change*; Stocker, T.F., Qin, D., Plattner, G.-K., Tignor, M., Allen, S.K., Boschung, J., Nauels, A., Xia, Y., Bex, V., Midgley, P.M., Eds.; Cambridge University Press: Cambridge, UK; New York, NY, USA, 2013; 126p.
28. Allen, R.G.; Pereira, L.S.; Raes, D.; Smith, M. *FAO Irrigation and Drainage Paper No. 56 Crop Evapotranspiration (Guidelines for Computing Crop Water Requirements)*; UN-FAO: Rome, Italy, 2006; p. 333.
29. Diedhiou, A.; Bichet, A.; Wartenburger, R.; Seneviratne, S.I.; Rowell, D.P.; Sylla, M.B.; Diallo, I.; Todzo, S.; Touré, N.d.E.; Camara, M.; et al. Changes in climate extremes over West and Central Africa at 1.5 °C and 2 °C global warming. *Environ. Res. Lett.* **2018**, *13*, 065020. [[CrossRef](#)]
30. Klutse, N.A.B.; Ajayi, V.; Gbobaniyi, E.O.; Egbebiyi, T.S.; Kouadio, K.; Nkrumah, F.; Quagraine, K.A.; Olusegun, C.; Diasso, U.J.; Abiodun, B.J.; et al. Potential impact of 1.5 °C and 2 °C global warming on consecutive dry and wet days over West Africa. *Environ. Res. Lett.* **2018**, *13*, 089502. [[CrossRef](#)]
31. Ali, H.; Mishra, V. Contrasting response of rainfall extremes to increase in surface air and dew point temperatures at urban locations in India. *Sci. Rep.* **2017**, *7*, 1–15. [[CrossRef](#)]
32. Nangombe, S.; Zhou, T.; Zhang, W.; Wu, B.; Hu, S.; Zou, L.; Li, D. Record-breaking climate extremes in Africa under stabilized 1.5 °C and 2 °C global warming scenarios. *Nat. Clim. Chang.* **2018**, *8*, 375–380. [[CrossRef](#)]
33. Lin, C.; Gentine, P.; Huang, Y.; Guan, K.; Kimm, H.; Zhou, S. Diel ecosystem conductance response to vapor pressure deficit is suboptimal and independent of soil moisture. *Agric. For. Meteorol.* **2018**, *250*, 24–34. [[CrossRef](#)]
34. Abiodun, B.J.; Makhanya, N.; Petja, B.; Abatan, A.A.; Oguntunde, P.G. Future projection of droughts over major river basins in Southern Africa at specific global warming levels. *Theor. Appl. Climatol.* **2019**, *137*, 1785. [[CrossRef](#)]



© 2019 by the authors. Licensee MDPI, Basel, Switzerland. This article is an open access article distributed under the terms and conditions of the Creative Commons Attribution (CC BY) license (<http://creativecommons.org/licenses/by/4.0/>).